THE JOURNAL OF PHYSICAL CHEMISTRY C

Article

pubs.acs.org/JPCC

Co-Sensitization of Zinc and Free-Base Porphyrins with an Organic Dye for Efficient Dye-Sensitized Solar Cells

Chin-Li Wang,[†] Jia-Wei Shiu,[‡] Yen-Ni Hsiao,[†] Pei-Shang Chao,[†] Eric Wei-Guang Diau,*[,‡] and Ching-Yao Lin*[,†]

[†]Department of Applied Chemistry, National Chi Nan University, Puli, Nantou 54561, Taiwan

[‡]Department of Applied Chemistry and Institute of Molecular Science, National Chiao Tung University, Hsinchu 30010, Taiwan

ABSTRACT: Co-sensitization of an efficient zinc porphyrin sensitizer (LD14) with its free-base analogue (H_2LD14) and an organic dye (AN-3) improves the efficiency of the dye-sensitized solar cells. The superior performance of the co-sensitized system is attributed to complementary absorptions of the three dyes, resulting in panchromatic incident photon-to-current conversion efficiency responses at the expense of only slightly lowered open-circuit voltage.

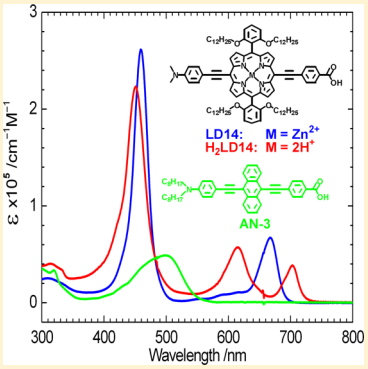

With the potential of becoming a clean and renewable energy source, dye-sensitized solar cells (DSSCs) have drawn much attention in recent years.[1−3] Porphyrins and their derivatives have been investigated as efficient sensitizers for DSSCs due to their vital roles in photosynthesis, strong absorption in the visible region, and the ease of adjusting their chemical structures for light harvest.[4−7] Since the pioneer work of Officer and co-workers in 2007 obtaining a power conversion efficiency (PCE) of 7.1%,[8−10] considerable efforts have been made[8−44] to raise the PCE to greater than 10% for a porphyrin-based DSSC.[11,15,26,36−38,41] Recently, Mathew et al. reported a porpyrin-based DSSC attaining a PCE of 13% using an SM315 porphyrin dye in a cobalt electrolyte.[43]

For most porphyrins, π-conjugation of the macrocyclic ring gives rise to two distinct absorptions in the UV−visible region, namely, the B (Soret) and Q bands, and leaves a gap between the two absorptions.[45] This intrinsic gap unfortunately limits the light-harvesting ability of the porphyrin dyes for DSSC applications. To remedy this problem, improved photovoltaic performance can be attained either by adjusting chemical structures of the dyes[43,44] or by employing a strategy of co-sensitization to fill the absorption gap.[9−12,28−34,39] Co-sensitization has been quite successful for many highly efficient porphyrin dyes.[11,14,41] In this work, we further extend such an approach by taking a previously reported, efficient zinc porphyrin sensitizer (LD14),[37,38] co-sensitized with its free-base analogue (H_2LD14), as well as an organic dye (AN-3), to achieve improved photovoltaic performance. Chart 1 depicts the chemical structures of these dyes. The purpose of combining these dyes in a co-sensitized film is to utilize their complementary absorption spectral features to achieve panchromatic light absorption and to extend light absorption into the near-IR region. As shown below in Figure 1, the B bands of H_2LD14 are slightly blue-shifted toward shorter wavelength from those of LD14. Significantly, the Q bands of H_2LD14 are split and distributed at both sides of the Q bands of LD14. These spectral differences are consistent with lowering the molecular symmetry of a porphyrin by removing the central metal ion.[45] Finally, the absorption bands of AN-3 locate around 500 nm, between the porphyrin B and Q bands. Similar to one of our co-sensitized systems,[41] the presence of this organic dye in the porphyrin system noticeably improves the overall performance of the DSSC.

Chart 1. Chemical Structures of the Porphyrins and Organic Dye in This Work: LD14, H_2LD14, and AN-3

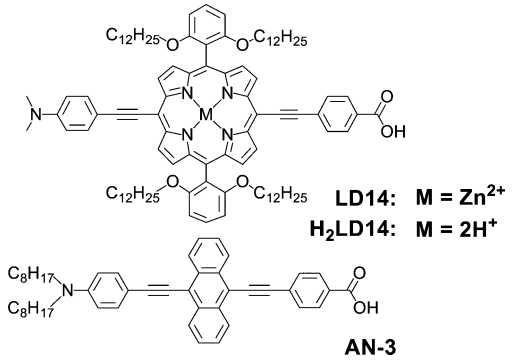

Received: October 5, 2014
Revised: November 9, 2014
Published: November 10, 2014

   dx.doi.org/10.1021/jp510057b | J. Phys. Chem. C 2014, 118, 27801−27807

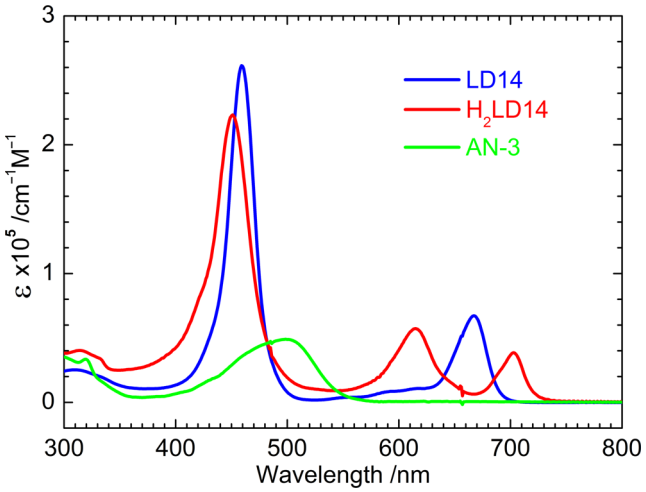

Figure 1. Absorption spectra of LD14, H_2LD14, and AN-3 dyes in THF.

EXPERIMENTAL SECTION

Synthesis and Characterization of Dyes. *Materials.* Air-sensitive solids were handled in a glovebox (MBraun Unilab). A vacuum line and standard Schlenk techniques were employed to process air-sensitive solutions. Solvents for the synthesis (ACS grade) were CH_2Cl_2 and $CHCl_3$ (Mallinckrodt Baker), hexanes (Haltermann, Hamburg, Germany), and THF (Merck, Darmstadt, Germany). These solvents were used as received unless otherwise stated. Other chemicals were obtained commercially (Acros Organics). THF for cross-coupling reactions was purified and dried with a solvent purification system (Asiawong SD-500, Taipei, Taiwan); about 50 ppm of H_2O was found in the resulting THF. For electrochemical measurements, THF was distilled over sodium under N_2. $Pd(PPh_3)_4$ catalyst (Strem) was used as received. For chromatographic purification, we used silica gel 60 (230−400 mesh, Merck).

Instruments. NMR spectra (Bruker Avance II 300 MHz NMR spectrometer at National Chi Nan University or Varian Inova 600 NMR spectrometer at National Chung Hsing University), elemental analyses (Elementar Vario EL III, Precision Instrumentation Center at National Taiwan University or MOST Instrumentation Center at National Chung Hsing University), mass spectra (Microflex MALDI-TOF MS, Bruker Daltonics), electrochemical measurements (CHI Electrochemical Workstation 611A), absorption spectra (Agilent 8453 UV−visible spectrophotometer), and fluorescence spectra (Varian Cary Eclipse fluorescence spectrometer) were recorded with the indicated instruments.

LD14. LD14 has been previously reported.[37]

H_2LD14. This free-base porphyrin is obtained by demetalating 130 mg of LD14 in 100 mL of $CHCl_3$ containing 10 mL of HCl (aq). The completeness of the reaction was verified by the UV−visible spectrum. After stirring for 4 h at room temperature, the solution was neutralized by adding 100 mL of Na_2CO_3 (aq). Be aware of massive CO_2 generation at this step. The organic layer was then washed with NH_4Cl (aq) and then H_2O, followed by filtration, and dried over Na_2SO_4, and $CHCl_3$ was removed under reduced pressure. The residual solid was then purified on a column chromatograph (silica gel) using CH_2Cl_2/MeOH = 9/1 as eluent. The product was collected after crystallization from CH_2Cl_2/MeOH at 67% yield. ^{1}H NMR (300 MHz, CDCl3 at 7.26 ppm): δ_H = 10.02 (s, 1H), 9.69 (d, J = 4.7 Hz, 2H), 9.16 (d, J = 4.6 Hz, 2H), 8.92 (d, J = 4.7 Hz, 2H), 8.86 (d, J = 4.6 Hz, 2H), 8.30 (d, J = 8.0 Hz, 2H), 8.10 (d, J = 8.3, 2H), 7.71 (t, J = 8.4 Hz, 2H), 7.01 (d, J = 8.4 Hz, 4H), 3.85 (t, J = 6.4 Hz, 8H), 1.29−1.01 (m, 26H), 1.00−0.88 (m, 17H), 0.82 (t, overlapped, J = 7.0 Hz, 21H), 0.72−0.61 (m, 9H), 0.60−0.39 (m, 25H), −2.4 (s, 2H). MALDI-TOF: m/z calcd for $C_{89}H_{122}N_4O_6$ 1342.94, found 1343.83, $[MH]^+$. Anal. Calcd for $C_{89}H_{122}N_4O_6$: C 79.54%, H 9.15%, N 4.17%. Found: C 79.23%, H 9.31%, N 3.82%.

AN-3. The synthetic procedure is illustrated below. The synthesis of compound **1** is based on the literature report.[46] For compound **2**, 380 mg of 9,10-dibromoanthracene (MW = 336.02 g/mol, 1.131 mmol) was usually mixed with 257.8 mg of compound **1** (MW = 341.57 g/mol, 0.755 mmol) in 30 mL of THF and 5 mL of triethylamine. After three cycles of freeze−pump−thaw, 87.3 mg of $Pd(PPh_3)_4$ (MW = 1156 g/mol, 7.55 × 10^{-2} mmol, 10 mol %) and 14.4 mg of CuI (MW = 190.45 g/mol,7.55 × 10^{-2} mmol, 10 mol %) were added to the solution under an inert atmosphere in a glovebox. The reaction was stirred at 70 °C for 24 h. The completion of the reaction was monitored by TLC. The solvent was removed by rotary evaporation. The residue was purified by column chromatography (silica gel) using CH_2Cl_2/n-hexanes = 1/4 as eluent to give compound **2** (MW = 596.68 g/mol) at 48.8% yield. For AN-3, 100 mg of compound **2** (MW = 596.68 g/mol, 0.168 mmol) was mixed with 73.5 mg of 4-ethynylbenzoic acid (MW = 146.14 g/mol, 3 equiv) in 30 mL of THF and 5 mL of triethylamine. After three cycles of freeze−pump−thaw, 29.1 mg of $Pd(PPh_3)_4$ (MW = 1156 g/mol, 2.52 × 10^{-2} mmol, 15 mol %) and 4.80 mg of CuI (MW = 190.45, 2.52 × 10^{-2} mmol, 15 mol %) were added to the solution under an inert atmosphere in a glovebox. The reaction was stirred at 40 °C for 38 h. The completion of the reaction was monitored by TLC. The solvent was removed by rotary evaporation. The residue was purified by column chromatography (silica gel) using MeOH/CH_2Cl_2 = 1/9 as eluent to get 79.0 mg of AN-3 (MW = 661.91 g/mol, yield = 71.0%). ^{1}H NMR (300 MHz, $CDCl_3$ at 7.26 ppm): δ_H 8.72 (d, J = 8.1 Hz, 2H), 8.65 (d, J = 8.1 Hz, 2H), 8.19 (d, J = 8.1 Hz, 2H), 7.86 (d, J = 8.3 Hz, 2H), 7.74−7.51 (m, 6H), 6.67 (d, J = 8.4 Hz, 2H), 3.32 (t, J = 7.4 Hz, 4H), 1.72−1.54 (br, 4H), 1.45−1.21 (br, 20H), 0.90 (t, J = 6.3 Hz, 6H). MALDI-TOF: m/z calcd for $C_{47}H_{51}NO_2$ 661.39, found 661.34 $[M]^+$. Anal. Calcd for $C_{47}H_{51}NO_2$·0.5H_2O: C 84.14%, H 7.81%, N 2.09%. Found: C 83.99%, H 7.77%, N 1.84%.

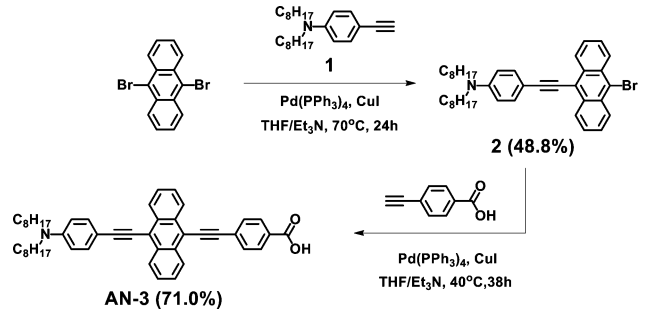

Device Fabrication and Characterizations. The DSSC devices were fabricated with a titania working electrode and a Pt-coated counter electrode in a sandwich-type structure. For the working electrode, octahedral TiO_2 nanocrystals (HD1) were synthesized using the hydrothermal methods reported elsewhere;[47] ethyl cellulose and α-terpineol were added to the

dx.doi.org/10.1021/jp510057b | J. Phys. Chem. C 2014, 118, 27801−27807

Table 1. Spectral and Electrochemical Data of LD14, H2LD14, and AN-3[a]

dyes	absorption λ_{max}/nm (log ε/M^{-1} cm^{-1})	emission[b] λ_{max}/nm	S^o/S^{+c}/eV	S*/eV	$E_{1/2}$/V vs SCE ox(1)	$E_{1/2}$/V vs SCE red(1)
LD14	459 (5.40), 667 (4.82)	682	−5.48	−3.64	+0.74	−1.32
H_2LD14	451 (5.35), 615 (4.76), 703 (4.59)	710	−5.59	−3.84	+0.85	−1.10
AN-3	499 (4.69)	603	−5.61	−3.33	+0.87[d]	−1.42

[a]Absorption and emission data were measured in THF at 25 °C. Electrochemical measurements were performed at 25 °C with each sample (0.5 mM) in THF/0.1 M TBAP/N_2, Pt working and counter electrodes, SCE reference electrode, scan rate = 100 mV s^{-1}. [b][sample] = 2×10^{-6} M in THF. Excitation wavelength/nm: LD14, 459; H_2LD14, 451; AN-3, 499. [c]S^o/S^+ values were estimated from the first oxidation potentials, $S^* = S^o/S^+ + E_{0-0}$. E_{0-0} values were estimated from the intersection of normalized UV−visible and fluorescent spectra. [d]Potential estimated by differential pulse voltammetry because the oxidation reaction is irreversible.

ethanol solution of these TiO_2 nanostructures to prepare a viscous paste suitable for screen-printing. The TiO_2 paste was then coated onto a $TiCl_4$-treated FTO glass substrate (TEC 7) to obtain a film of thickness 19 μm with repetitive screen-printing. The film thickness of a scattering layer was 8 μm and the active size of the device was 0.4 × 0.4 cm^2. The TiO_2 films were then annealed according to a programmed procedure. The annealed films were treated with fresh $TiCl_4$ aqueous solution (40 mM) at 70 °C for 30 min and sintered at 500 °C for 30 min. The dye uptake of LD14 was performed by soaking the TiO_2 films in a solution of toluene and ethanol (v/v = 1/1, [LD14] = 0.15 mM) at 25 °C for 2−3 h. For the co-sensitized system, the two-dye cocktail solution contained LD14 (0.1 mM) and H2LD14 (0.1 mM), and the three-dye cocktail solution contained LD14 (0.1 mM), H_2LD14 (0.05 mM), and AN-3 (0.05 mM). The counter electrode was made by spin-coating the H_2PtCl_6/2-propanol solution onto a FTO glass substrate through a typical procedure of thermal decomposition. The two electrodes were assembled into a sandwich-type cell and sealed with a spacer of thickness 40 μm. The electrolyte injected into the device contained I_2 (0.05 M), LiI (0.1 M), 1-methyl-3-propylimidazolium iodide (PMII) (1.0 M), and 4-*tert*-butylpyridine (0.5 M) in a cosolvent containing acetonitrile and valeronitrile with a volume ratio of 85/15.

The current−voltage (J−V) characteristics of the DSSC devices covered with a black mask (aperture area 0.45 × 0.45 cm^2) were determined with a solar simulator (AM 1.5G, XES-40S1, SAN-EI). The spectra of incident photon-to-current conversion efficiency (IPCE) of the corresponding devices were measured with a system comprising a Xe lamp (A-1010, PTi, 150 W), monochromator (PTi, 1200 gr mm^{-1} blazed at 500 nm), and source meter (Keithley 2400). The measurements of intensity-modulated photovoltage spectra (IMVS) and charge extraction (CE) were carried out with CIMPS instruments (Zahner) reported elsewhere.[48]

RESULTS AND DISCUSSION

Optical and Electrochemical Properties. The UV−visible absorption spectra of LD14, H_2LD14, and AN-3 in THF are compared in Figure 1. The peak absorption coefficients and the corresponding wavelengths are collected in Table 1. The absorption bands of H_2LD14 are found at 451, 615, and 703 nm. Due to the lowered molecular symmetry and lack of a central metal ion, the B bands of H_2LD14 are slightly broadened and blue-shifted from those of LD14, whereas the Q bands of H_2LD14 are split into two groups of absorptions, residing at both the red- and blue-sides of the Q bands of LD14. For AN-3, the absorption bands locate at 499 nm, which is between the porphyrin B and Q bands. As such, the absorption spectra of LD14, H_2LD14, and AN-3 complement each other very well. Figure 2 shows the fluorescence spectra of LD14, H_2LD14, and AN-3 in THF. The emission maxima are

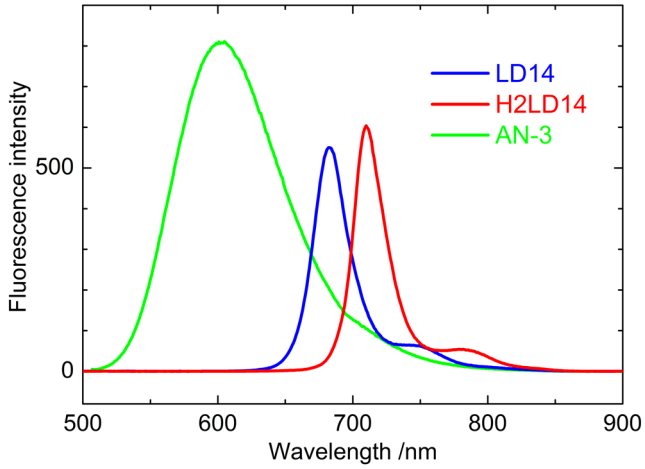

Figure 2. Fluorescence emission spectra of LD14, H_2LD14, and AN-3 dyes in THF (2×10^{-6} M).

listed in Table 1. As shown in the figure, the emission bands of H_2LD14, LD14, and AN-3 are located at 710, 682, and 603 nm, respectively. Apparently, the emission bands of H_2LD14 are more red-shifted than those of LD14 and AN-3. This phenomenon is consistent with the spectral features of the dyes shown in the absorption spectra. It is worthy to note that the fluorescent emission of AN-3 extends up to 800 nm, overlapping with the Q-band absorptions of LD14 and H_2LD14. This implies that energy transfer from AN-3 to the porphyrins may be possible.

For the redox properties, the cyclic voltammograms of LD14, H_2LD14, and AN-3 are compared in Figure 3. The redox potentials are summarized in Table 1. For the reductions, the first porphyrin ring reductions of LD14 and H_2LD14 as well as the first reduction of AN-3 are all quasi-reversible reactions at −1.32, −1.10, and −1.42 V vs SCE, respectively. On the other hand, the first oxidations of LD14 and H_2LD14 are observed as quasi-reversible reactions at +0.74 and +0.85 V vs SCE, respectively. AN-3, however, demonstrates an irreversible oxidation reaction. Therefore, the differential pulse voltammogram of AN-3 was carried out to help estimate the oxidation potential (+0.87 V vs SCE).

Figure 4 shows the energy-level diagram of LD14, H_2LD14, and AN-3, comparing the ground-to-oxidized state (S^o/S^+) and the first singlet excited state (S*) of each dye, the conduction bands (CB) of TiO_2, and the redox potential of I^-/I^{3-}. The first oxidation potentials were used to estimate the S^o/S^+ levels. The

dx.doi.org/10.1021/jp510057b | J. Phys. Chem. C 2014, 118, 27801−27807

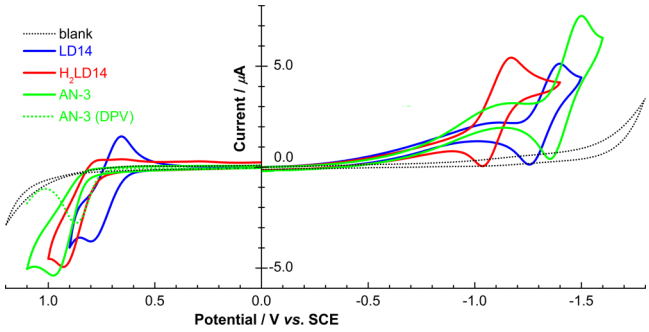

Figure 3. Cyclic voltammograms of 1.0 mM LD14, H_2LD14, and AN-3 dyes in THF/0.1 M TBAP. (The dotted green line represents the differential pulse voltammogram of AN-3.)

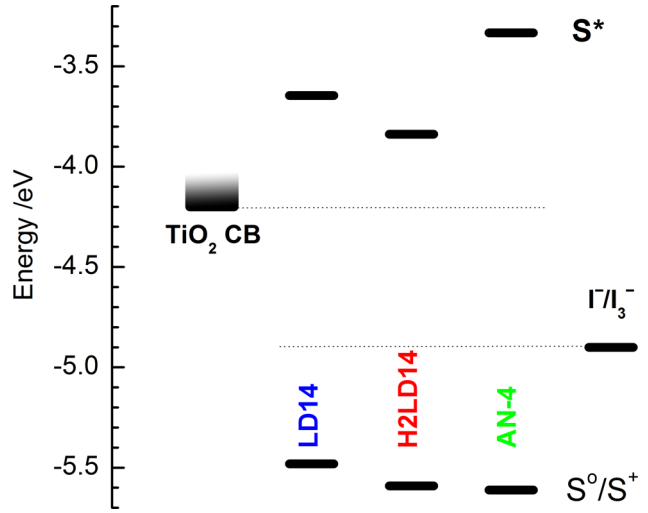

Figure 4. Energy levels of LD14, H_2LD14, and AN-4 vs those of TiO_2 conduction bands and the electrolyte.

zero−zero excitation energies obtained from the intersection of the corresponding normalized absorption and emission spectra were used to estimate the energy gaps between the S* and the S^o/S^+ levels. As shown in the diagram, all dyes in this study should be capable of injecting electrons to the CB of TiO_2 upon excitation, and the resulting cations can be efficiently regenerated by the electrolyte.

Photovoltaic Properties. Five systems are tested for their photovoltaic performance: (1) LD14 alone, (2) H_2LD14 alone, (3) AN-3 alone, (4) LD14 co-sensitized with H_2LD14, and (5) LD14 co-sensitized with H_2LD14 and AN-3. Parts a and b of Figure 5 show the $J-V$ curves and the corresponding IPCE spectra of these systems, respectively. The photovoltaic parameters are summarized in Table 2. The results of charge extraction (CE) and intensity-modulated photovoltage spectroscopy (IMVS) measurements are shown in Figure 6.

For the single-dye devices, LD14 clearly outperforms H_2LD14 and AN-3. For H_2LD14, the poorer performance may be related to the lower energy level of the excited state (Figure 4). This may result in less favorable electron-injection and is consistent with the smaller IPCE values (Figure 5b). The inferior performance of the AN-3 cell may be related to the narrower absorption spectral range and the lower extinction coefficient of the dye (Figure 2). Light harvesting limited in a narrower region may lead to poorer photovoltaic performance.

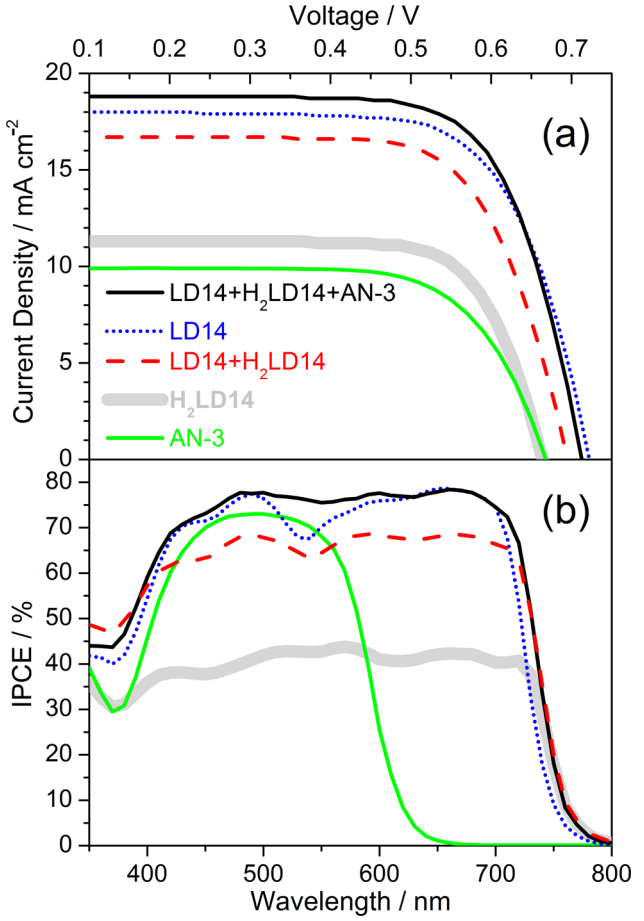

Figure 5. (a) $J-V$ characteristics and (b) IPCE spectra of the devices made of LD14, H_2LD14, AN-3 and the co-sensitized systems.

Table 2. Photovoltaic Properties of Porphyrins LD14, H_2LD14, AN-3 and the Co-Sensitized Systems[a]

dyes	J_{sc}/mA cm^{-2}	V_{oc}/mV	FF/%	η/%
LD14	18.035	727	70.61	9.25
H_2LD14	11.389	668	73.86	5.62
AN-3	9.912	672	70.27	4.68
LD14/H_2LD14	16.714	698	71.27	8.31
LD14/H_2LD14/AN-3	18.760	716	72.29	9.72

[a]All TiO_2 working electrodes were fabricated under the same experimental conditions; the photovoltaic parameters were obtained under simulated AM-1.5G illumination (power density 100 mW·cm^{-2}) and active area 0.16 cm^2 with a black mask of area 0.2025 cm^2.

For the co-sensitized systems, the LD14/H_2LD14 cell shows poorer V_{oc} and J_{sc} values than those of the LD14 cell. The lower V_{oc} could be related to the lower S* level of H_2LD14 than that of LD14. This is consistent with the potential shift of conduction band edge shown in Figure 6a. The weaker J_{sc} of the LD14/H_2LD14 cell compared to that of the LD14 cell is consistent with its generally smaller IPCE values across the action spectrum shown in Figure 5b. Nevertheless, the IPCE spectrum of the LD14/H_2LD14 device exhibits broader spectral response in the near-IR region. In addition, the spectral dip between the B and Q bands around 540 nm is less apparent for the LD14/H_2LD14 co-sensitized system than for the LD14-alone cell. These phenomena could be due to (i) complementary absorption bands of AN-3, LD14, and H_2LD14 and

dx.doi.org/10.1021/jp510057b | J. Phys. Chem. C 2014, 118, 27801−27807

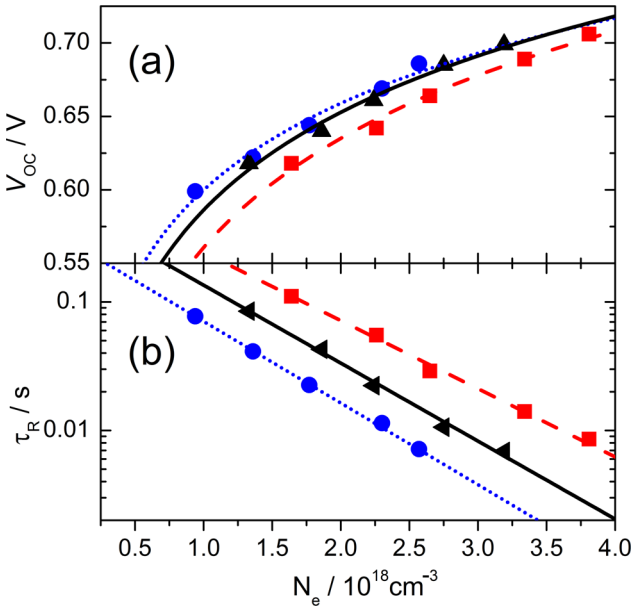

Figure 6. Plots of (a) V_{OC} vs charge density (N_e) and (b) electron lifetime (τ_R) vs N_e for the devices made of LD14 alone (circles) and LD14 + H_2LD14 (squares) and the LD14 + H_2LD14 + AN-3 (triangles) co-sensitized systems.

(ii) the split and more red-shifted Q bands of H_2LD14. Significantly, the LD14/H_2LD14/AN-3 system outperforms the other systems with J_{sc} = 18.76 mA cm^{-2}, V_{oc} = 716 mV, FF = 0.72%, and an overall device efficiency η = 9.72%. With the presence of the AN-3 dye, the V_{oc} of the LD14/H_2LD14/AN-3 device is greater than that of the LD14/H_2LD14 cell. This is consistent with the upward potential shift shown in Figure 6a. Although the electron lifetime (τ_R) of the LD14/H_2LD14 system was retarded (Figure 6b), the V_{oc} indicates that the position of the potential band edge is the dominated factor to be considered. As a result, the V_{oc} of the LD14/H_2LD14/AN-3 device is close to that of the LD14 cell and significantly larger than that of the LD14/H_2LD14 system. The J_{sc} of the LD14/H_2LD14/AN-3 system is clearly the largest among the others. The greater J_{sc} is consistent with the IPCE spectra showing a panchromatic feature on light-harvesting ability of this three-dye co-sensitized system.

CONCLUSIONS

In this work, we demonstrated that the photovoltaic performance of a DSSC could be improved in a co-sensitized system containing a zinc porphyrin (LD14), its free-base analogue (H_2LD14), and an organic dye (AN-3). The co-sensitization of a zinc porphyrin with a free-base porphyrin takes advantage of their complementary UV−visible absorptions as well as the red-shifting features of the Q bands of a free-base porphyrin dye. The presence of AN-3 organic dye considerably improves the photovoltaic performance of the co-sensitized system and fills up the gap between the Soret and Q bands of the pophyrins in the IPCE spectrum. The three-dye co-sensitized system showed an improved overall efficiency (9.72%), outperforming those of the LD14 cell (9.25%) and the LD14/H_2LD14 system (8.31%).

AUTHOR INFORMATION

Corresponding Authors

*E.W.-G.D.: fax, +886-3-5723764; tel, +886-3-5131524; e-mail, diau@mail.nctu.edu.tw.

*C.-Y.L.: fax, +886-49-2917956; tel, +886-49-2910960, ext. 4152; e-mail: cyl@ncnu.edu.tw.

Notes

The authors declare no competing financial interest.

ACKNOWLEDGMENTS

This work is supported by the Ministry of Science and Technology, Taiwan.

ABBREVIATIONS USED

DSSC, dye-sensitized solar cell; PCE, power conversion efficiency; IPCE, incident photon-to-electron conversion efficiency; CE, charge extraction; IMVS, intensity-modulated photovoltage spectroscopy.

REFERENCES

(1) Grätzel, M. Photoelectrochemical Cells. *Nature* **2001**, *414*, 338−344.

(2) O'Regan, B.; Grätzel, M. A Low-Cost, High-Efficiency Solar Cell Based on Dye-Sensitized Colloidal TiO_2 Films. *Nature* **1991**, *353*, 737−740.

(3) Hamann, T. W.; Ondersma, J. W. Dye-Sensitized Solar Cell Redox Shuttles. *Energy Environ. Sci.* **2011**, *4*, 370−381.

(4) Campbell, W. M.; Burrell, A. K.; Officer, D. L.; Jolley, K. W. Porphyrins as Light Harvesters in the Dye-Sensitised TiO_2 Solar Cell. *Coord. Chem. Rev.* **2004**, *248*, 1363−1379.

(5) Imahori, H.; Umeyama, T.; Ito, S. Large π-Aromatic Molecules as Potential Sensitizers for Highly Efficient Dye-Sensitized Solar Cells. *Acc. Chem. Res.* **2009**, *42*, 1809−1818.

(6) Li, L.-L.; Diau, E. W.-G. Porphyrin-Sensitized Solar Cells. *Chem. Soc. Rev.* **2013**, *42*, 291−304.

(7) Imahori, H.; Kurotobi, K.; Walter, M. G.; Rudine, A. B.; Wamser, C. C. *Handb. Porphyrin Sci.* **2012**, *18*, 57−121.

(8) Campbell, W. M.; Jolley, K. W.; Wagner, P.; Wagner, K.; Walsh, P. J.; Gordon, K. C.; Schmidt-Mende, L.; Nazeeruddin, M. K.; Wang, Q.; Grätzel, M.; Officer, D. L. Highly Efficient Porphyrin Sensitizers for Dye-Sensitized Solar Cells. *J. Phys. Chem. C* **2007**, *111*, 11760−11762.

(9) Griffith, M. J.; Mozer, A. J.; Tsekouras, G.; Dong, Y.; Wagner, P.; Wagner, K.; Wallace, G. G.; Mori, S.; Officer, D. L. Remarkable Synergistic Effects in a Mixed Porphyrin Dye-Sensitized TiO_2 Film. *Appl. Phys. Lett.* **2011**, *98*, 163502−163505.

(10) Griffith, M. J.; Sunahara, K.; Wagner, P.; Wagner, K.; Wallace, G. G.; Officer, D. L.; Furube, A.; Katoh, R.; Mori, S.; Mozer, A. J. Porphyrins for Dye-Sensitised Solar Cells: New Insights into Efficiency-Determining Electron Transfer Steps. *Chem. Commun.* **2012**, *48*, 4145−4162.

(11) Yella, A.; Lee, H.-W.; Tsao, H. N.; Yi, C.; Chandiran, A. K.; Nazeeruddin, M. K.; Diau, E. W.-G.; Yeh, C.-Y.; Zakeeruddin, S. M.; Grätzel, M. Porphyrin-Sensitized Solar Cells with Cobalt (II/III)-Based Redox Electrolyte Exceed 12% Efficiency. *Science* **2011**, *334*, 629−634.

(12) Bessho, T.; Zakeeruddin, S. M.; Yeh, C.-Y.; Diau, E. W.-G.; Grätzel, M. Highly Efficient Mesoscopic Dye-Sensitized Solar Cells Based on Donor−Acceptor-Substituted Porphyrins. *Angew. Chem., Int. Ed.* **2010**, *49*, 6646−6649.

(13) Mai, C.-L.; Huang, W.-K.; Lu, H.-P.; Lee, C.-W.; Chiu, C.-L.; Liang, Y.-R.; Diau, E. W.-G.; Yeh, C.-Y. Synthesis and Characterization of Diporphyrin Sensitizers for Dye-Sensitized Solar Cells. *Chem. Commun.* **2010**, *46*, 809−811.

(14) Wu, H.-P.; Ou, Z.-W.; Pan, T.-Y.; Lan, C.-M.; Huang, W.-K.; Lee, H.-W.; Reddy, N. M.; Chen, C.-T.; Chao, W.-S.; Yeh, C.-Y.; Diau, E. W.-G. Molecular Engineering of Cocktail Co-Sensitization for Efficient Panchromatic Porphyrin-Sensitized Solar Cells. *Energy Environ. Sci.* **2012**, *5*, 9843−9848.

(15) Kurotobi, K.; Toude, Y.; Kawamoto, K.; Fujimori, Y.; Ito, S.; Chabera, P.; Sundström, V.; Imahori, H. Highly Asymmetrical

Porphyrins with Enhanced Push−Pull Character for Dye-Sensitized Solar Cells. *Chem.—Eur. J.* **2013**, *19*, 17075−17081.
(16) Ye, S.; Kathiravan, A.; Hayashi, H.; Tong, Y.; Infahsaeng, Y.; Chabera, P.; Pascher, T.; Yartsev, A. P.; Isoda, S.; Imahori, H.; Sundström, V. Role of Adsorption Structures of Zn−Porphyrin on TiO_2 in Dye-Sensitized Solar Cells Studied by Sum Frequency Generation Vibrational Spectroscopy and Ultrafast Spectroscopy. *J. Phys. Chem. C* **2013**, *117*, 6066−6080.
(17) Ishida, M.; Hwang, D.; Koo, Y. B.; Sung, J.; Kim, D. Y.; Sessler, J. L.; Kim, D. *β*-(Ethynylbenzoic Acid)-Substituted Push−Pull Porphyrins: DSSC Dyes Prepared by a Direct Palladium-Catalyzed Alkynylation Reaction. *Chem. Commun.* **2013**, *49*, 9164−9166.
(18) Lee, C. Y.; She, C.; Jeong, N. C.; Hupp, J. T. Porphyrin Sensitized Solar Cells: TiO_2 Sensitization with a *π*-Extended Porphyrin Possessing Two Anchoring Groups. *Chem. Commun.* **2010**, *46*, 6090−6092.
(19) Hamann, T. W.; Jensen, R. A.; Martinson, A. B. F.; Ryswykac, H. V.; Hupp, J. T. Advancing Beyond Current Generation Dye-Sensitized Solar Cells. *Energy Environ. Sci.* **2008**, *1*, 66−78.
(20) Rangan, S.; Coh, S.; Bartynski, R. A.; Chitre, K. P.; Galoppini, E.; Jaye, C.; Fischer, D. Energy Alignment, Molecular Packing, and Electronic Pathways: Zinc(II) Tetraphenylporphyrin Derivatives Adsorbed on $TiO_2(110)$ and $ZnO(11\bar{2}0)$ Surfaces. *J. Phys. Chem. C* **2012**, *116*, 23921−23930.
(21) Pellejà, L.; Kumar, C. V.; Clifford, J. N.; Palomares, E. D−*π*−A Porphyrin Employing an Indoline Donor Group for High Efficiency Dye-Sensitized Solar Cells. *J. Phys. Chem. C,* **2014**, *118*, 16504−16509.
(22) Kang, M. S.; Kang, S. H.; Kim, S. G.; Choi, I. T.; Ryu, J. H.; Ju, M. J.; Cho, D.; Lee, J. Y.; Kim, H. K. Novel D−*π*−A Structured Zn(II)-Porphyrin Dyes Containing a Bis(3,3-dimethylfluorenyl)amine Moiety for Dye-Sensitized Solar Cells. *Chem. Commun.* **2012**, *48*, 9349−9351.
(23) Kang, S. H.; Choi, I. T.; Kang, M. S.; Eom, Y. K.; Ju, M. J.; Hong, J. Y.; Kang, H. S.; Kim, H. K. Novel D−*π*−A Structured Porphyrin Dyes with Diphenylamine Derived Electron-Donating Substituents for Highly Efficient Dye-Sensitized Solar Cells. *J. Mater. Chem. A* **2013**, *1*, 3977−3982.
(24) Choi, I. T.; Ju, M. J.; Kang, S. H.; Kang, M. S.; You, B. S.; Hong, J. Y.; Eom, Y. K.; Song, S. H.; Kim, H. K. Structural Effect of Carbazole-Based Coadsorbents on the Photovoltaic Performance of Organic Dye-Sensitized Solar Cells. *Mater. Chem. A* **2013**, *1*, 9114−9121.
(25) Choi, I. T.; Kim, Y. W.; You, B. S.; Kang, S. H.; Hong, J. Y.; Ju, M. J.; Kim, H. K. Novel D−*π*−A Structured Zn(II)−Porphyrin Dyes with Bulky Fluorenyl Substituted Electron Donor Moieties for Dye-Sensitized Solar Cells. *J. Mater. Chem. A* **2013**, *1*, 9848−9852.
(26) Luo, J.; Xu, M.; Li, R.; Huang, K.-W.; Jiang, C.; Qi, Q.; Zeng, W.; Zhang, J.; Chi, C.; Wang, P.; Wu, J. N-Annulated Perylene as an Efficient Electron Donor for Porphyrin-Based Dyes: Enhanced Light-Harvesting Ability and High-Efficiency Co(II/III)-Based Dye-Sensitized Solar Cells. *J. Am. Chem. Soc.* **2014**, *136*, 265−272.
(27) Jiao, C.; Zu, N.; Huang, K.-W.; Wang, P.; Wu, J. Perylene Anhydride Fused Porphyrins as Near-Infrared Sensitizers for Dye-Sensitized Solar Cells. *Org. Lett.* **2011**, *13*, 3652−3655.
(28) He, H.; Gurung, A.; Sia, L.; Sykes, A. G. A Simple Acrylic Acid Functionalized Zinc Porphyrin for Cost-Effective Dye-Sensitized Solar Cells. *Chem. Commun.* **2012**, *48*, 7619−7621.
(29) Shrestha, M.; Si, L.; Chang, C.-W.; He, H.; Sykes, A.; Lin, C.-Y.; Diau, E. W.-G. Dual Functionality of BODIPY Chromophore in Porphyrin-Sensitized Nanocrystalline Solar Cells. *J. Phys. Chem. C* **2012**, *116*, 10451−10460.
(30) Chang, S.; Wang, H.; Hua, Y.; Li, Q.; Xiao, X.; Wong, W.-K.; Wong, W. Y.; Chen, X. Z.; Conformational, T. Engineering of Co-Sensitizers to Retard Back Charge Transfer for High-Efficiency Dye-Sensitized Solar Cells. *J. Mater. Chem. A* **2013**, *1*, 11553−11558.
(31) Liu, Y.; Lin, H.; Dy, J. T.; Tamaki, K.; Nakazaki, J.; Nakayama, D.; Uchida, S.; Kubo, T.; Segawa, H. *N*-Fused Carbazole-Zinc Porphyrin-Free-Base Porphyrin Triad for Efficient Near-IR Dye-Sensitized Solar Cells. *Chem. Commun.* **2011**, *47*, 4010−4012.
(32) Liu, Y.; Lin, H.; Li, J.; Dy, J. T.; Tamaki, K.; Nakazaki, J.; Nakayama, D.; Nishiyama, C.; Uchida, S.; Kubo, T.; Segawa, H. Ethynyl-Linked Push−Pull Porphyrin Hetero-Dimers for Near-IR Dye-Sensitized Solar Cells: Photovoltaic Performances versus Excited-State Dynamics. *Phys. Chem. Chem. Phys.* **2012**, *14*, 16703−16712.
(33) Wang, Y.; Chen, B.; Wu, W.; Li, X.; Zhu, W.; Tian, H.; Xie, Y. Efficient Solar Cells Sensitized by Porphyrins with an Extended Conjugation Framework and a Carbazole Donor: From Molecular Design to Cosensitization. *Angew. Chem., Int. Ed.* **2014**, *53*, 10779−10783.
(34) Mojiri-Foroushani, M.; Dehghani, H.; Salehi-Vanani, N. Enhancement of Dye-Sensitized Solar Cells Performances by Improving Electron Density in Conduction Band of Nanostructure TiO_2 Electrode with Using a Metalloporphyrin as Additional Dye. *Electrochim. Acta* **2013**, *92*, 315−322.
(35) Lin, C.-Y.; Lo, C.-F.; Luo, L.; Lu, H.-P.; Hung, C.-S.; Diau, E. W.-G. Design and Characterization of Novel Porphyrins with Oligo(phenylethylnyl) Links of Varied Length for Dye-Sensitized Solar Cells: Synthesis and Optical, Electrochemical, and Photovoltaic Investigation. *J. Phys. Chem. C* **2009**, *113*, 755−764.
(36) Wang, C.-L.; Chang, Y.-C.; Lan, C.-M.; Lo, C.-F.; Diau, E. W.-G.; Lin, C.-Y. Enhanced Light Harvesting with *π*-Conjugated Cyclic Aromatic Hydrocarbons for Porphyrin-Sensitized Solar Cells. *Energy Environ. Sci.* **2011**, *4*, 1788−1795.
(37) Chang, Y.-C.; Wang, C.-L.; Pan, T.-Y.; Hong, S.-H.; Lan, C.-M.; Kuo, H.-H.; Lo, C.-F.; Hsu, H.-Y.; Lin, C.-Y.; Diau, E. W.-G. A Strategy To Design Highly Efficient Porphyrin Sensitizers for Dye-Sensitized Solar Cells. *Chem. Commun.* **2011**, *47*, 8910−8912.
(38) Wang, C.-L.; Lan, C.-M.; Hong, S.-H.; Wang, Y.-F.; Pan, T.-Y.; Chang, C.-W.; Kuo, H.-H.; Kuo, M.-Y.; Diau, E. W.-G.; Lin, C.-Y. Enveloping Porphyrins for Efficient Dye-Sensitized Solar Cells. *Energy Environ. Sci.* **2012**, *5*, 6933−6940.
(39) Lan, C.-M.; Wu, H.-P.; Pan, T.-Y.; Chang, C.-W.; Chao, W.-S.; Chen, C.-T.; Wang, C.-L.; Lin, C.-Y.; Diau, E. W.-G. Enhanced Photovoltaic Performance with Co-Sensitization of Porphyrin and an Organic Dye in Dye-Sensitized Solar Cells. *Energy Environ. Sci.* **2012**, *5*, 6460−6464.
(40) Wu, C.-H.; Chen, M.-C.; Su, P.-C.; Kuo, H.-H.; Wang, C.-L.; Lu, C.-Y.; Tsai, C.-H.; Wu, C.-C.; Lin, C.-Y. Porphyrins for Efficient Dye-Sensitized Solar Cells Covering the Near-IR Region. *J. Mater. Chem. A* **2014**, *2*, 991−999.
(41) Wang, C.-L.; Hu, J.-Y.; Wu, C.-H.; Kuo, H.-H.; Chang, Y.-C.; Lan, Z.-J.; Wu, H.-P.; Diau, E. W.-G.; Lin, C.-Y. Highly Efficient Porphyrin-Sensitized Solar Cells with Enhanced Light Harvesting Ability Beyond 800 nm and Efficiency Exceeding 10%. *Energy Environ. Sci.* **2014**, *7*, 1392−1396.
(42) Ball, J. M.; Davis, N. K. S.; Wilkinson, J. D.; Kirkpatrick, J.; Teuscher, J.; Gunning, R.; Anderson, H. L.; Snaith, H. J. A Panchromatic Anthracene-Fused Porphyrin Sensitizer for Dye-Sensitized Solar Cells. *RSC Adv.* **2012**, *2*, 6846−6853.
(43) Mathew, S.; Yella, A.; Gao, P.; Humphry-Baker, R.; Curchod, B. F. E.; Ashari-Astani, N.; Tavernelli, I.; Rothlisberger, U.; Nazeeruddin, M. K.; Grätzel, M. Dye-Sensitized Solar Cells with 13% Efficiency Achieved Through the Molecular Engineering of Porphyrin Sensitizers. *Nat. Chem.* **2014**, *6*, 242−247.
(44) Yella, A.; Mai, C.-L.; Zakeeruddin, S. M.; Chang, S.-N.; Hsieh, C.-H.; Yeh, C.-Y.; Grätzel, M. Molecular Engineering of Push−Pull Porphyrin Dyes for Highly Efficient Dye-Sensitized Solar Cells: The Role of Benzene Spacers. *Angew. Chem., Int. Ed.* **2014**, *53*, 2973−2977.
(45) Gouterman, M. Spectra of Porphyrins. *J. Mol. Spectrosc.* **1961**, *6*, 138−163.
(46) Zeitouny, J.; Aurisicchio, C.; Bonifazi, D.; Zorzi, R. D.; Geremia, S.; Bonini, M.; Palma, C.-A.; Samorı, P.; Listorti, A.; Belbakra, A.; Armaroli, N. Photoinduced Structural Modifications in Multicomponent Architectures Containing Azobenzene Moieties as Photoswitchable Cores. *J. Mater. Chem.* **2009**, *19*, 4715−4724.
(47) Shiu, J.-W.; Lan, C.-M.; Chang, Y.-C.; Wu, H.-P.; Huang, W.-K.; Diau, E. W.-G. Size-Controlled Anatase Titania Single Crystals with

Octahedron-like Morphology for Dye-Sensitized Solar Cells. *ACS Nano* **2012**, *6*, 10862−10873.
(48) Li, L.-L.; Chang, Y.-C.; Wu, H.-P.; Diau, E. W.-G. Characterisation of Electron Transport and Charge Recombination Using Temporally Resolved and Frequency-Domain Techniques for Dye-Sensitised Solar Cells. *Int. Rev. Phys. Chem.* **2012**, *31*, 420−467.